

Enhancement of flux pinning and high critical current density in graphite doped MgB₂ superconductor

Chandra Shekhar^{a)}, Rajiv Giri, R. S. Tiwari and O. N. Srivastava^{a)}

Department of Physics Banaras Hindu University, Varanasi-221005, India

S. K. Malik

Tata Institute of Fundamental Research, Mumbai-400005, India

ABSTRACT

We report the synthesis and characterization of graphite (C) doped MgB_{2-x}C_x (x = 0.0, 0.1, 0.2 and 0.3) samples. The crystal structure and microstructural characterization have been investigated by x-ray diffractometer and transmission electron microscopic (TEM) analysis. The superconducting properties especially J_c and H_{c2} have been measured by employing physical property measurement system. We found that the graphite doping affects the lattice parameters as well as the microstructure of MgB₂ superconductor. In case of optimally doped (x = 0.1) sample, the critical current density at 5K corresponds to 1.1×10^6 and 5.3×10^4 A/cm² for 3T and 5T fields respectively. The upper critical field has been enhanced nearly two times after doping. The flux pinning behavior has been investigated by flux pinning force density curve and it reveals that the flux pinning behaviour has improved significantly by doping. TEM micrographs show the graphite nanoparticles of size ~5-10 nm which are invariably present in MgB₂ grains. These nanoparticles act as flux pinning centre and are responsible for enhancement of superconducting properties of MgB₂.

^{a)}e-mail: hepons@yahoo.com (O N Srivastava), chand_bhu@yahoo.com (Chandra Shekhar)
Phone & Fax: +91 542 2369889

INTRODUCTION

After the discovery of superconductivity in MgB₂¹, considerable effort has been made to improve the critical current density (J_c), upper critical field (H_{c2}) and irreversibility field (H_{irr}) of this superconductor. The absence of weak links at grain boundaries in MgB₂^{2,3} makes it easier to improve superconducting abilities by introducing additional pinning centres in MgB₂ superconductor. Doping of elements or compounds has been found to be effective for improving the superconducting properties of bulk, tapes, wires and films especially under magnetic fields. The enhanced properties of above mentioned form of MgB₂ superconductor are well above those of standard high field materials e.g. Nb-based superconductor⁴. This raises the possibility of using MgB₂ as replacement of Nb-based superconductors. Large number of dopants e.g. carbon⁵⁻¹¹ as well as carbon containing compounds, SiC¹²⁻¹⁹, B₄C²⁰⁻²² carbohydrate²³ and aromatic hydrocarbon²⁴ have been reported to be effective for enhancement of superconducting properties such as H_{irr} , H_{c2} and J_c under higher magnetic field. In these cases, doping of carbon and carbon containing compound resulted in the substitution of carbon at boron site and introduction of nonsuperconducting particles, which provide effective flux pinning centres and resulted in significant enhancement of H_{c2} and J_c ²⁵⁻²⁹. Reduction of coherence length due to enhanced impurity scattering is considered to contribute to the enhancement of H_{c2} ³⁰⁻³³. Furthermore, flux pinning strength was found to be enhanced by carbon substitution^{6,19,20,23,24}. These positive effects of carbon substitution indicate that doping of carbon has a great potential to enhance superconducting properties of MgB₂ superconductor. Although most of earlier investigations are related to the effect of carbon substitution on the superconducting properties of MgB₂, relatively sparse studies have been carried out on the microstructures of doped MgB₂^{10,11}. However, the arrangement of carbon atoms in graphite (C) sheet is somewhat similar to the arrangement of B atoms in MgB₂, studies on graphite

doping is of special significance. The earlier reports present only comparison of SiC, C₆₀, CNT and graphite doping on J_c in MgB₂^{34,35}. In order to enhance the value of J_c and H_{c2} , however, investigation pertaining to optimization of size of carbon nanoparticles and their homogeneous distribution in the superconductor would be required. In the present work the effect of graphite doping on superconducting properties like, T_c , J_c , H_{c2} and H_{irr} of MgB₂ superconductor have been carried out. We have studied the effect of graphite doping on the crystal lattice, superconducting properties and their correlation with microstructures of MgB₂ superconductor which have been prepared by encapsulation method developed by us^{36,37}. In the present work, we have evaluated T_c , J_c , H_{c2} , H_{irr} and bulk flux pinning force density (F_p) from magnetization measurement of undoped and doped MgB₂ superconductors. The structural and microstructural properties have been carried out employing powder x-ray diffraction (XRD) and transmission electron microscopy (TEM) technique in diffraction and imaging modes.

EXPERIMENTAL DETAILS

The synthesis of graphite doped MgB₂ samples with stoichiometric ratio MgB_{2-x}C_x (x = 0.0, 0.1, 0.2 and 0.3) have been carried out by solid state reaction method at ambient pressure by employing a special encapsulation technique^{36,37} developed in our laboratory. Magnesium Mg (purity - 99.9%, size - 30-40μm), amorphous boron B (purity - 99%, size - 5-6μm) and graphite C (purity - 99.9%, size 40-50 nm) were fully mixed and cold pressed into small rectangular pellets (10x5x1) mm³. The pellets were encapsulated with Mg metal cover to take care of Mg loss and avoid the formation of MgO during sintering process. The pellet configuration was rapped in a Ta foil and sintered in flowing high purity Ar gas in a programmable tube type furnace at 900°C for 2 hours. The pellets were cooled to room temperature at the rate of 5°C /min. The encapsulating Mg cover was removed and pellets were retrieved for further study.

All the samples were subjected to crystal structure characterization by powder x-ray diffraction technique (XRD, PANalytical X' Pert Pro, $\text{CuK}\alpha$ radiation with $\lambda = 1.5406 \text{ \AA}$) and microstructural characterization by transmission electron microscopy (TEM, Philips-CM-12). Magnetization measurements have been done by physical property measurement system (PPMS, Quantum Design, TIFR Mumbai, India) on pellet of diameter and length 1.2 mm 4 mm respectively of as synthesized MgB_2 samples over a temperature range of 5-50K. The J_c of pellet samples was calculated by using Bean's formula based on critical state model³⁸.

$$J_c = \frac{30\Delta M}{\langle d \rangle}$$

where ' ΔM ' (emu/cm^2) is the height of hysteresis loop and ' $\langle d \rangle$ ' (cm) is the diameter of pellet which is used in magnetization measurement.

RESULTS & DISCUSSION

Fig (1) shows XRD patterns of $\text{MgB}_{2-x}\text{C}_x$ samples for $x = 0.0, 0.1, 0.2$ and 0.3 . Excepting peaks at 26.2° and 52.4° , all peaks are identified by MgB_2 compound with space group $\text{P6}/\text{mmm}$. These additional two peaks are identified as (002) and (004) reflections of graphite. The intensity of these peaks increases with doping as shown in Fig. 1(b, c & d) and no other impurity phase such as MgB_2C_2 has been found²¹. This XRD pattern reveals that the undoped and doped MgB_2 samples are polycrystalline in nature. XRD analysis using a computerized programme based on least square fitting method gives lattice parameters $a = 3.078 \text{ \AA}$ and $c = 3.522 \text{ \AA}$ for pure MgB_2 sample. It is very close to the standard values³⁹. We have noticed the shift in the positions of (100) and (002) peaks corresponding to MgB_2 phase with increasing concentration of graphite. The position of the (100) peak is shifted to higher angles with increasing level of doping, indicating a decrease in the ' a ' lattice parameter as shown in Fig. 2(a). However, the position of the (002) peak has only slightly changed with increasing doping^{9,10,30} as shown in Fig. 2(b). As can be seen in Fig 2(c), the in-plane lattice parameter ' a ' decreases from 3.078 to 3.051 \AA and lattice parameter ' c ' from 3.522 to 3.523 \AA for doping $x = 0.2$. This can be understood because the average size of C atom ($r_C = 0.772 \text{ \AA}$) is smaller than that of B atom ($r_B = 0.822 \text{ \AA}$). The change in lattice parameters indicates that C atom is substituted in the boron honeycomb layer in the MgB_2 crystal. Furthermore, doping was also confirmed by analysis of full width at half maximum (FWHM) values for peaks (100), (101), (002) and (110) as shown in Fig 2(d). The broadening in diffraction line has also increased with doping. Broadening in peaks in present investigation is likely to arise from lattice strain mainly caused by doping on B sites. It may be noted that decrease in grain size could also result in peak broadening. However, by SEM investigation, the grain size seemed to remain the same for all samples.

The magnetic susceptibility (χ) of $\text{MgB}_{2-x}\text{C}_x$ ($x = 0.0, 0.1, 0.2$ and 0.3) samples are shown in Fig. (3)

as a function of temperature. Based on this, the transition temperature of pure and doped MgB_2 with different concentration can be taken to lie between 34-40K. The T_c decreases with increasing doping concentration. Most importantly, the pure MgB_2 has T_c at 40K while the doped material has T_c ranging from 36-34 K. Thus doped samples show somewhat lower but still sharp T_c . The T_c drops only 4K²¹ for $x = 0.1$ suggesting that only a small amount of C atom has substituted at B site in our samples.

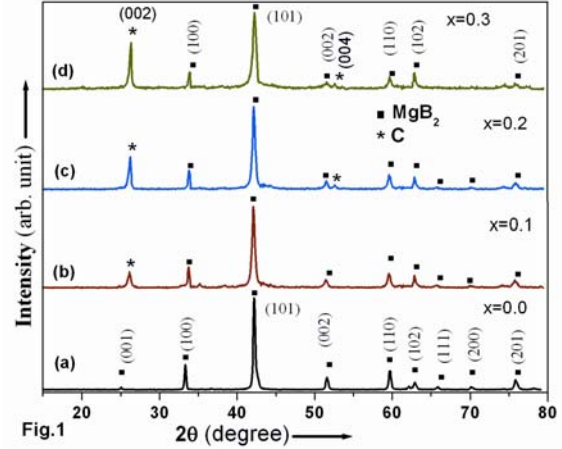


FIG.1. (Color) Representative powder XRD patterns of $\text{MgB}_{2-x}\text{C}_x$ (a) $x = 0.0$, (b) $x = 0.1$, (c) $x = 0.2$ and (d) $x = 0.3$.

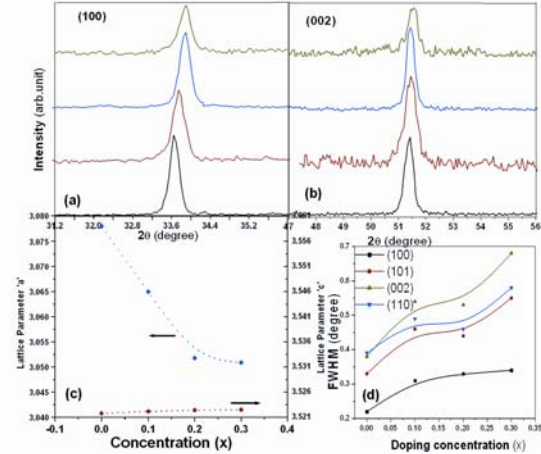


FIG.2. (Color) (a) & (b) show the magnified view of the XRD patterns corresponding to (100) and (002) reflections respectively (c) shows change in lattice parameters with doping concentration (d) shows the variation in FWHM of (100), (101), (002) and (110) reflections with doping concentration.

the magnetization measurements as function of applied magnetic field have been carried out at 5, 10, 20 and 30 K for each sample. The dependence of J_c on the applied magnetic field is shown in Fig. (4). It is clear from figure that the J_c value for $x = 0.1$ sample attains the highest value among all the samples for temperatures upto 30 K and fields upto 6T. For example the J_c value at 5K for optimally doped sample (i.e. $x = 0.1$) is $8.4 \times 10^6 \text{ A/cm}^2$ in self field, $1.1 \times 10^6 \text{ A/cm}^2$ at 3T and $5.3 \times 10^4 \text{ A/cm}^2$ at 5T. On the other hand the J_c value of pure sample is 2.4×10^5

A/cm² in self field, 1.3×10^4 A/cm² at 3T and 2.9×10^2 A/cm² at 5T at 5K. Based on MgB₂ superconductor, most of devices can operate at 20K where as conventional superconductor can not operate due to low T_c .

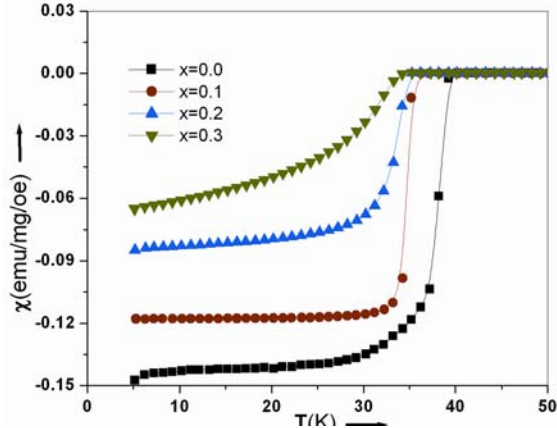


FIG.3. (Color) Temperature dependent dc magnetic susceptibility (χ) behavior of MgB_{2-x}C_x for $x = 0.0, 0.1, 0.2$ and 0.3 .

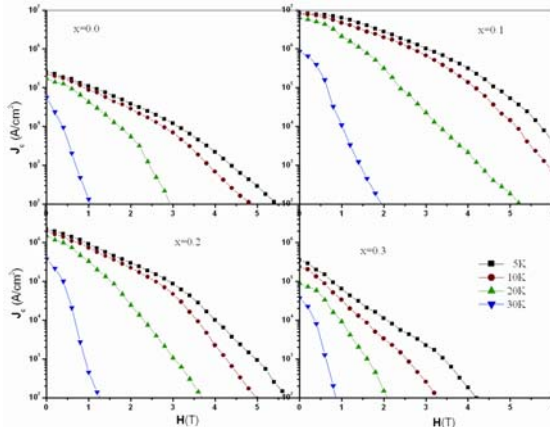


FIG.4. (Color) Critical current density J_c as a function of applied magnetic field for MgB_{2-x}C_x (a) $x = 0.0$, (b) $x = 0.1$, (c) $x = 0.2$ and (d) $x = 0.3$ at 5, 10, 20 and 30K.

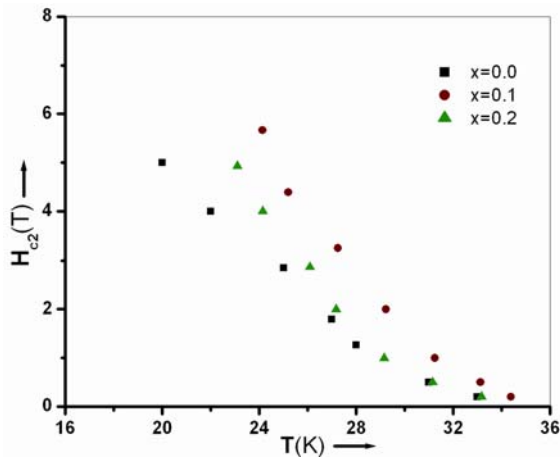


FIG.5. (Color) The upper critical field as a function of temperature for MgB_{2-x}C_x, $x = 0.0, 0.1, 0.2$ doped samples.

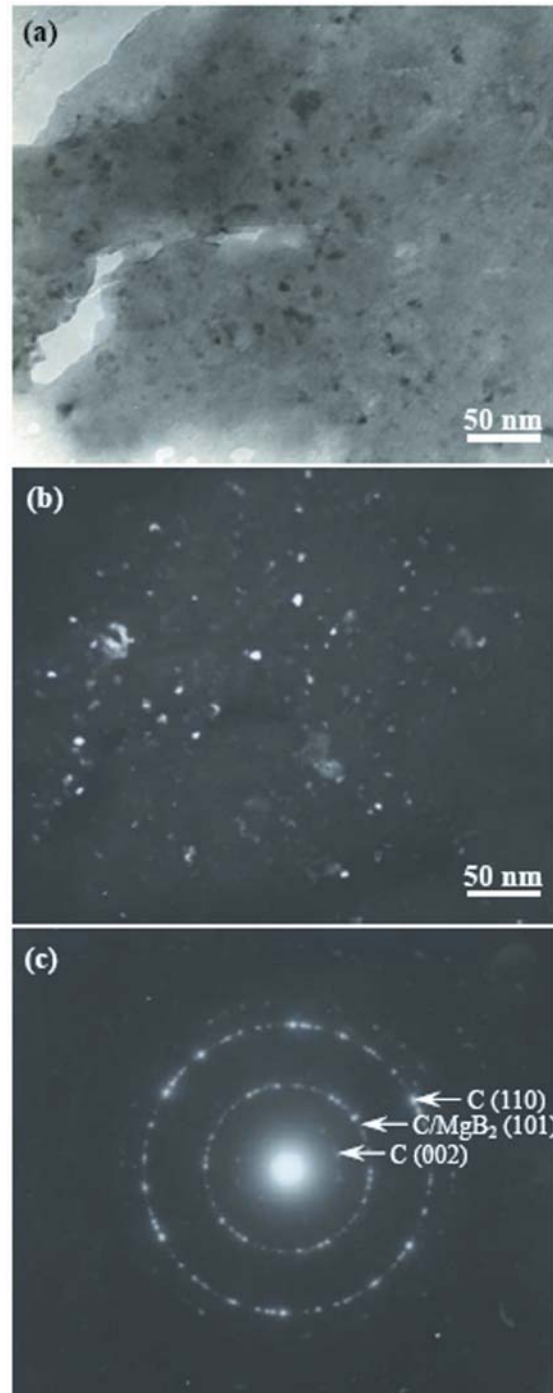


FIG.6. (Color) The representative TEM image of MgB_{2-x}C_x with $x = 0.1$. (a) the bright field image shows presence of graphite nanoparticles (b) the dark field image of same region i.e. (a). This image also shows the presence of graphite nanoparticles in MgB₂ grain. (c) the selected area diffraction (SAD) pattern corresponding to image (a) shows spotty rings which have been identified as due to graphitic phase of carbon.

Therefore, J_c value of optimally doped MgB₂ sample $x = 0.1$ at 20K is $3.2 \times 10^5, 2.3 \times 10^4$ and 2.2×10^3 A/cm² at 2T, 3T and 4T respectively. These values are significantly higher as compared to recent work done

on MgB_2 ^{34,35,40-41}. The above values clearly show that doping has resulted in enhancement of J_c for all fields.

We have done the isofield magnetization measurements as a function of temperature between 5 to 50K and noted the superconducting transition temperature at field 0.2, 0.5, 1, 2, 3, 4 and 5T. These superconducting transition temperature values are used to plot the $H_{c2}(T)$ versus temperature on horizontal axis as shown in Fig (5). The extrapolation of curve gives the H_{c2} value at 0K. The value of H_{c2} at 0K for pure MgB_2 sample is 16T and for $x = 0.1$ and $x = 0.2$ MgB_2 samples are 33T and 23.1T respectively. These values are also close to the values obtained by Werthamer Helfand-Hoheberg Model⁴².

$$H_{c2}(0) = 0.7T_c \left[\frac{dH_{c2}}{dT} \right]$$

which yields 17T, 31T and 25T as $H_{c2}(0)$ values for $x = 0$, $x = 0.1$ and $x = 0.2$ respectively. The enhancements of H_{c2} suggest that the doping of graphite in MgB_2 induces disorder and results in shortening of electronic mean free path. The selective tuning of impurity scattering may improve the H_{c2} value of MgB_2 superconductor. These values are comparable to recent work done by Pallecchi et al⁴³. They have studied the effect of neutron irradiation on H_{c2} values of MgB_2 . The H_{c2} values obtained in their experiment are also in agreement with the model of two band impurity^{44,45}. It appears that graphite impurity in MgB_2 grain is enhancing the band scattering leading to increased H_{c2} values.

Since the central aim of present investigation is to explore the enhanced superconducting properties of doped MgB_2 samples and their possible correlation with microstructural features, we have carried out investigations of microstructural features induced by doping of different concentration of doping in MgB_2 . Fig. 6 (a) shows the bright field TEM micrograph for doped sample ($x = 0.1$). From this micrograph the presence of nanoparticles is easily discernible. Fig 6(b) shows dark field TEM image of same region [i.e. Fig. 6(a)] which confirms the presence of nanoparticles in MgB_2 grain. Fig. 6(c) shows the selected area diffraction (SAD) pattern corresponding to Fig. 6(a). The SAD pattern reveals the spotty rings which have been identified as due to graphitic phase of carbon. From Fig. 6(a, b & c) it can be easily concluded that the nanoparticles invariably present in MgB_2 grain are graphite nanoparticles. These particles are distributed homogeneously in MgB_2 grain. The size of nanoparticles has been found to be in the range of ~5-10 nm. It is interesting to note that some concentration of graphite have gone to honey comb layer on B site in MgB_2 ³⁰ (as it is evident from XRD analysis) and remaining concentration of graphite in the form of nanoparticles has been identified by TEM analysis. It may be pointed out that the microstructure of doped MgB_2 in the present case shows uniformly distributed graphitic nanoparticles only where as several other phases have been reported as inclusion particles by Yanwei et al¹¹. This difference may be due to differences in method of sample preparation in two cases. Furthermore, the size and distribution of

inclusion particles are more close to coherence length for MgB_2 in comparison to the inclusion of MgAg and LaB_6 reported in earlier studies^{36,37}

In order to get broad insight of pinning mechanism, we have calculated values of H_{irr} for undoped and doped MgB_2 samples using Kramer Scaling law⁴⁷. We have plotted the values of $J_c^{0.5} H^{0.25}$ versus H for temperatures 5, 10, 20 and 30 K. A straight line has been found at each temperature for H ($H \geq 0.5T$) as can be seen in Fig. 7 (a,b&c). The values of H_{irr} can be determined by extrapolating the straight line toward horizontal axis^{2,5}. We have determined the value of H_{irr} for different concentration of doping and undoped samples at different temperature as shown in fig. 7(d). We have used these values of H_{irr} for further analyzing the shape of flux pinning force density F_p versus reduced field H^* (H/H_{irr}) curves.

Flux pinning mechanism associated with microstructural defects is assessed by analyzing the shape of F_p curve as a function of applied field and temperature. It is expected that if pinning is arising due to grain boundary, F_p will exhibit $H^{*0.5}(1-H^*)^2$ dependence⁴⁶. For analyzing the shape of F_p curve, the normalized pinning force $f = F_p/F_{pmax}$ is plotted against reduced field H^* for different concentration of doping. The curve overlap, when a single pinning mechanism and centre is considered to be involved⁴⁷ i.e. grain boundaries alone act as pinning centres. Such scaling behaviour is commonly observed in Nb-based superconductors⁴⁸. We have plotted f versus H^* curves for pure and doped MgB_2 samples at temperature 5, 10, 20 and 30K as shown in Fig. (8). For the pure MgB_2 samples, the best fit is found for

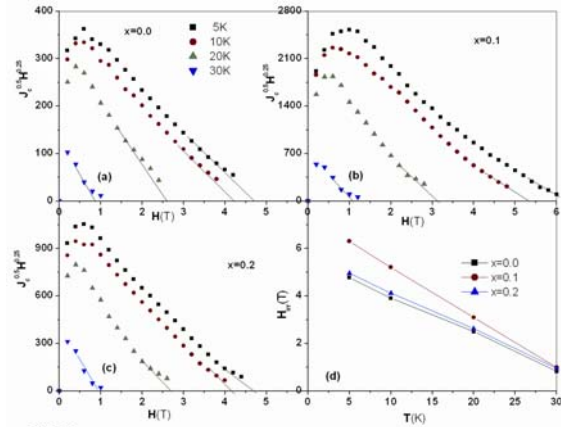


FIG. 7. (Color) The variation of $J_c^{0.5} H^{0.25}$ with magnetic field H for (a) $x = 0.0$, (b) $x = 0.1$, (c) $x = 0.2$ at temperatures 5, 10, 20 and 30 K (d) shows the variation of H_{irr} (it is deduced after extrapolating curves in (a), (b) & (c)) with temperature.

$H^{*0.5}(1-H^*)^2$ which is attributed to grain boundary pinning⁴⁶. A similar observation has also been reported in pure polycrystalline bulk MgB_2 sample². For $x = 0.1$ doped sample, the shape of the curve has significantly broadened and peak is shifted to higher H^* value. This indicates that the nanoparticles inclusion has provided extra pinning centres³⁶. Colley et al have

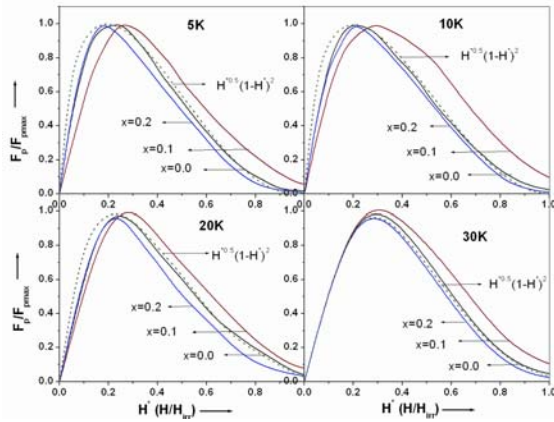


FIG.8. (Color) Normalized pinning force F_p/F_{pmax} as a function of reduced magnetic field H/H_{irr} at (a) 5K, (b) 10K, (c) 20K and (d) 30K of $MgB_{2-x}C_x$ for $x = 0.0, 0.1, 0.2$

found similar shift for carbon doping in $MgCNi_3$ superconductor and they have attributed this shift to core pinning by carbon nanoparticles⁴⁹. When graphite concentration is high i.e. $x > 0.1$ the flux pinning force behaviour is suppressed. However, it may be pointed out that the result on the types of pinning based on figures 7 & 8 has some ambiguity. It only broadly indicates that the optimally doped MgB_2 sample shows high pinning strength at larger reduced magnetic fields.

CONCLUSION

Based on the above results it can be concluded that we have synthesized successfully graphite doped MgB_2 superconductor by solid state reaction method employing encapsulation technique. The lattice parameters have changed noticeably due to the substitution of C atom in honeycomb layer of B in MgB_2 crystal. For optimally doped ($x = 0.1$) MgB_2 significant enhancement in the superconducting properties such as J_c , H_{c2} and H_{irr} have been found. Despite of some ambiguity in the shape of flux pinning force density curve, it may be concluded that the flux pinning strength is enhanced at higher magnetic fields in optimally graphite doped sample. TEM microstructures clearly show the presence of graphite nanoparticles (size $\sim 5-10$ nm) embedded in the MgB_2 grains. It may further be concluded that these nanoparticles having size comparable to the coherence length ($\sim 5-6$ nm) of MgB_2 superconductor are responsible for the effective flux pinning and consequently enhancing the superconducting properties.

ACKNOWLEDGEMENTS

The authors are grateful to Prof. A.R. Verma, Prof. C.N.R. Rao, Prof. S.K. Joshi and Prof. A.K. Roychaudhary for fruitful discussion and suggestions. Financial supports from UGC, DST-UNANST and CSIR are gratefully acknowledged. One of the authors (C. S.) is thankful to UGC New Delhi, Government of India for awarding senior project fellowship.

REFERENCES

1. J. Nagamatsu, N. Norimasa, T. Muranaka, Y. Zenitani and J. Akimitsu, Nature **410**, 63 (2001).
2. D. C. Larbalestier et al, Nature **410**, 186 (2001).
3. A. V. Pan, S.i Zhou, H. Liu and S. Dou, Supercond. Sci. Technol. **16**, 639 (2003).
4. Y. Iwasa, D.C Larbalestier, M. Orada, R Penco. M. D. Sumpston and X. Xi, Appl. Supercond. **16**, 1457 (2006).
5. J. Chen et al, Phys. Rev. B **74**, 174511 (2006).
6. C. Krutzler, M. Zehetmayer, M. Eisterer, H. W. Weber, N. D. Zhigadlo, J. Karpinski, and A. Wisniewski, Phys. Rev. B **74**, 144511 (2006).
7. X. Huang, W. Mickelson, B.C. Regan and A. Zettl, Solid State Commun. **136**, 278 (2005).
8. B. J. Senkowicz, J. E. Giencke, S. Patnaik, C. B. Eom, E. E. Hellstrom, and D. C. Larbalestier, Appl. Phys. Lett. **86**, 202502 (2005).
9. S. M. Kazakov, R. Puzniak, K. Rogacki, A. V. Mironov, N. D. Zhigadlo, J. Jun, Ch. Soltmann, B. Batlogg, and J. Karpinski, Phys. Rev. B **71**, 024533 (2005).
10. A. V. Pogrebnyakov et al, Appl. Phys. Lett. **85**, 2017 (2004).
11. Y. Ma, X. Zhang, G. Nishijima, K. Watanabe, S. Awaji and X. Bai, Appl. Phys. Lett. **88**, 072502 (2006).
12. O. Shcherbakova, S. X. Dou, S. Soltanian, D. Wexler, M. Bhatia, M. Sumpston, and E.W.Collings, J. Appl. Phys. **99**, 08M510 (2006).
13. Y. Wang, G. A. Voronin, T. W. Zerda and A. Winiarski, J. Phys.: Condens. Matter **18**, 275 (2006).
14. S. X. Dou, V. Braccini, S. Soltanian, R. Klie, Y. Zhu, S. Li, X. L. Wang and D. Larbalestier, J. Appl. Phys. **96**, 7549 (2004).
15. S. X. Dou et al, Appl. Phys. Lett. **81**, 3419 (2002).
16. W Pachla et al, Supercond. Sci. Technol. **19**, 1(2006).
17. S. K. Chen, K. S. Tan, B. A. Glowacki, W. K. Yeoh, S. Soltanian, J. Horvat, and S. X. Dou Appl. Phys. Lett. **87**, 182504 (2005).
18. O. V. Shcherbakova, A. V. Pan, S. Soltanian, S. X. Dou and D. Wexler Supercond. Sci. Technol. **20**, 5 (2007).
19. A. Matsumoto, H. Kumakura, H. Kitaguchi, B. J. Senkowicz, M. C. Jewell, E. E. Hellstrom, Y. Zhu, P. M. Voyles, and D. C. Larbalestier, Appl. Phys. Lett. **89**, 132508 (2006).
20. P. Lezza, C. Senatore and R. Flükiger, Supercond. Sci. Technol. **19**, 1030 (2006).
21. W. Mickelson, J. Cumings, W. Q. Han, and A. Zettl, Phys. Rev. B **65**, 052505 (2002).
22. A. Yamamoto, J. Shimoyama, S. Ueda, I. Iwayama, S.Horii and K. Kishio Supercond. Sci. Technol. **18**, 1323 (2005).

23. J. H. Kim, S. Zhou, M. S. A. Hossain, A. V. Pan, and S. X. Dou, *Appl. Phys. Lett.* **89**, 142505 (2006).
24. H. Yamada, M. Hirakawa, H. Kumakura and H. Kitaguchi, *Supercond. Sci. Technol* **19**, 175 (2006).
25. S. K. Chen, M. Wei, and J. L. MacManus-Driscoll, *Appl. Phys. Lett.* **88**, 192512 (2006).
26. X. L. Wang, Z. X. Cheng, and S. X. Dou, *Appl. Phys. Lett.* **90**, 042501 (2007).
27. C. H. Jiang, T. Nakane and H. Kumakura, *Supercond. Sci. Technol.* **18**, 902 (2005).
28. X. Zhang, Y. Ma, Z. Gao, Z. Yu, G. Nishijima and K. Watanabe, *Supercond. Sci. Technol.* **19**, 699 (2006).
29. A. Yamamoto, J. Shimoyama, S. Ueda, S. Horii, and K. Kishio, *Appl. Supercond.* **16**, 1411 (2006).
30. R. H. T. Wilke, S. L. Bud'ko, P. C. Canfield, D. K. Finnemore, Raymond J. Suplinskas and S. T. Hannahs *Phys. Rev. Lett.* **92**, 217003 (2004).
31. T. Masui, S. Lee, and S. Tajima *Phys. Rev. B* **70**, 024504 (2004)
32. S. M. Kazakov, R. Puzniak, K. Rogacki, A. V. Mironov, N. D. Zhigadlo, J. Jun, Ch. Soltmann, B. Batlogg, and J. Karpinski, *Phys. Rev. B* **71**, 024533 (2005).
33. C. Krutzler, M. Zehetmayer, M. Eisterer, H. W. Weber, N. D. Zhigadlo, J. Karpinski, and A. Wisniewski, *Phys. Rev. B* **74**, 144511 (2006).
34. P. Kováč, I. Hušek, V. Skákalova, J. Meyer, E. Dobročka, M. Hirscher and S. Roth, *Supercond. Sci. Technol.* **20**, 105(2007).
35. K. Agatsuma, M. Furuse, M. Umeda, S. Fuchino, W. J. Lee, and J. M. Hur, *IEEE Trans Appl. Supercond.* **16**, 1407 (2006).
36. C. Shekhar, R. Giri, R. S. Tiwari, S. K. Malik and O. N. Srivastava, *J Appl Phys*, **101**, 043906 (2007).
37. C. Shekhar, R. Giri, R. S. Tiwari, D. S. Rana, S. K. Malik and O. N. Srivastava, *Supercond. Sci. Technol.* **18**, 1210 (2005).
38. C.P.Bean, *Rev. Mod. Phys.* **36**, 31 (1964).
39. M. E. Jones, R. E. Marsh, *J. Am. Chem. Soc.* **76**, 1434 (1954).
40. Y. Zhao, Y. Feng, T. M. Shen, G. Li, Y. Yang and C. H. Cheng, *J. Appl. Phys.* **100**, 123902 (2006).
41. Y. Ma et al, *Supercond. Sci. Technol.* **19**, 133 (2006).
42. E. Helfand and N. R. Werthamer, *Phys. Rev.* **147**, 288 (1996).
43. I. Pallecchi et al, *Phys. Rev. B* **71**, 212507 (2005).
44. A. Gurevich, *Phys. Rev. B* **67**, 184515 (2003).
45. V. Braccini et al, *Phys. Rev. B* **71**, 012504 (2005).
46. E. J. Krammer, *J. Appl. Phys.* **44**, 1360 (1973).
47. W. A. Fietz and W. W. Webb, *Phy. Rev.* **178**, 657(1969).
48. C. Meingast and D. C. Larbalestier, *J. Appl. Phys.* **66**, 5971(1989).
49. L. D. Cooley, X. Song, J. Jiang, D. C. Larbalestier T. He, K. A. Regan, and R. J. Cava, *Phys. Rev. B* **65**, 214518 (2002).